Eur. Phys. J. B **28**, 121–128 (2002)
DOI: 10.1140/epjb/e2002-00208-8

THE EUROPEAN PHYSICAL JOURNAL B

Current and shot noise in two capacitively coupled single electron transistors with an atomic sized spacer

G. Michałek[a] and B.R. Bułka

Institute of Molecular Physics, Polish Academy of Sciences, ul.Smoluchowskiego 17, 60–179 Poznań, Poland

Received 9 October 2001 / Received in final form 8 March 2002
Published online 9 July 2002

Abstract. The currents and their fluctuations in two capacitively coupled single electron transistors are determined in the limit of sequential tunnelling. Our considerations are restricted to the case when the islands (dots) of the transistors are atomic–sized, which means each of them has only one single electronic level available for the tunnelling processes. The Coulomb interactions of accumulated charges on the both single electron transistors lead to the effect of the negative differential resistance. An enhancement of the current shot–noise was also found. Spectral decomposition analysis indicated the two main contributions to the shot–noise: low– and high–frequency fluctuations. It was found that the low frequency fluctuations (polarization noise) are responsible for a strong enhancement of the current noise.

PACS. 73.23.Hk Coulomb blockade; single-electron tunnelling – 73.40.Gk Tunnelling – 73.50.Td Noise processes and phenomena

1 Introduction

Recent progresses in modern photolithography and self–assembly techniques allows the fabrication of molecular–scale tunnel junction devices [1]. The small size and low power dissipation have stimulated a number of proposals for their use in future generations of computation technology, but until now few such circuits have been realised.

One of the most interesting type of tunnel junctions is the single–electron transistor (SET). In electrical devices consisting of two such structures connected in parallel, one can observe the negative differential resistance effect (NDR), which appears due to the Coulomb interaction of charges accumulated on both dots [2]. The NDR phenomenon is important in the case of potential applications such as amplifiers, mixers, multipliers, logic and memory elements, analog to digital converters and high–frequency oscillator circuits.

A very important parameter, with regard to the potential applications, is the noise to signal ratio. Besides thermal and $1/f$ noise, a *shot noise* also appears in electrical devices [3,4]. The shot noise analysis gives us additional information about the dynamics of the system, in particular about an electronic structure and electron–electron correlation, which cannot be obtained by conductance measurements. Extensive research of the shot noise in mesoscopic systems has been undertaken over the last fifteen years. It was shown that a correlation between the conducting electrons is responsible for the reduction of the shot noise below the Poissonian value (for uncorrelated electron transmission) $S_{\rm Poisson} = 2eI$ in quantum point contacts, metallic diffusive conductors, chaotic cavities and other devices (see review [4]). The reduction of the shot noise in the single–electron transistor (SET) (up to a value of $(1/2)S_{\rm Poisson}$) was confirmed experimentally in 1995 [5]. In some cases however the shot noise can also be much enhanced above the Poissonian value. In 1998, super–Poissonian noise was measured in a resonant tunnelling diode in the NDR regime [6].

To the best our knowledge, there has been neither theoretical nor experimental work reported on the shot noise in molecular–scale systems. Our purpose is to study the negative differential resistance phenomenon and the shot noise in such a system. As we will show, the NDR effect appears due to the Coulomb interactions of charge accumulated on both the transistors. We will also perform the spectral decomposition analysis of the shot noise to find processes, which are responsible for the super–Poissonian type of the current noise.

The paper is organized as follows; the formalism used for calculating the electric current, its fluctuation and other characteristics of the system, will be described in Section 2. In Section 3 we will present results of our calculation, and a summary including the final remarks are given in Section 4.

2 Description of the model

We consider a system, which is composed of two single electron transistors (SETs) connected in parallel (Fig. 1), with an atomic–sized spacer (dot). The crucial role in the device plays the Coulomb interaction between charges localized on both dots and the electrodes (dot–dot and

[a] e-mail: grzechal@ifmpan.poznan.pl

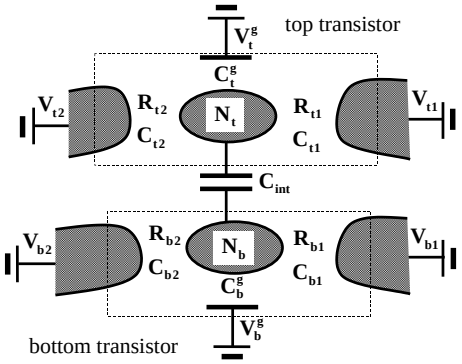

Fig. 1. Schematic view of two capacitively coupled single–electron transistors. Each dot α ($\alpha \in \{t, b\}$) is connected to two electrodes, labelled i ($i \in \{1, 2\}$). The dot–dot and dot–electrode Coulomb interactions are modelled by the capacitances C_{int} and $C_{\alpha i}$, respectively. The tunnelling through the junction αi depend on the resistance $R_{\alpha i}$, while N_t (N_b) denotes the number of excess electrons on the top (bottom) dot.

dot–electrode interactions). To investigate this situation we can introduce a simple formalism, based on the Hubbard model for the interaction of electrons in narrow energy bands [7]. The significant difference between the Hubbard Hamiltonian [7] and our model is related to the fact that we neglect all quantum–mechanical correlation terms, like exchange interactions, due to the limit of sequential tunnelling. In this way, the system may be described by the following Hamiltonian

$$\mathcal{H} = \mathcal{H}_{dot} + \mathcal{H}_{d-l} + \mathcal{H}_{d-d} \,, \tag{1}$$

where $\mathcal{H}_{dot}$ represents electrons on the dots, whilst $\mathcal{H}_{d-l}$ represents electrons in the electrodes and dot–electrode Coulomb interactions, as well as electron tunnelling. The last term $\mathcal{H}_{d-d}$ represents the Coulomb interaction between the dots. The dots' Hamiltonian $\mathcal{H}_{dot}$ can be divided into two parts

$$\mathcal{H}_{dot} = \sum_{\alpha,\sigma} (\epsilon_\alpha - eV_\alpha^g) c_{\alpha\sigma}^\dagger c_{\alpha\sigma} + \sum_\alpha U_\alpha n_{\alpha\uparrow} n_{\alpha\downarrow},$$

where $c_{\alpha\sigma}^\dagger$ and $c_{\alpha\sigma}$ are the creation and annihilation operators for an electron of spin projection $\sigma \in \{\uparrow, \downarrow\}$ on dot $\alpha \in \{t, b\}$, and $n_{\alpha\sigma} = c_{\alpha\sigma}^\dagger c_{\alpha\sigma}$ is the number operator. The first term describes electrons on the isolated dot with level ϵ_α (shifted by the external gate voltage V_α^g). The second refers to the Coulomb interaction between electrons of opposite spins on the same dot. The Hamiltonian

$$\mathcal{H}_{d-l} = \sum_{\alpha,i,k,\sigma} [\xi_{\alpha ik} + eV_{\alpha i}] d_{\alpha ik\sigma}^\dagger d_{\alpha ik\sigma} + \sum_{\alpha,i,k,\sigma} U_{\alpha i} n_{\alpha\sigma} n_{\alpha ik\sigma} + \sum_{\alpha,i,k,\sigma} (T_{\alpha i} c_{\alpha\sigma}^\dagger d_{\alpha ik\sigma} + \text{h.c.})$$

consists of three parts. The first term describes the noninteracting electrons in the electrodes, labelled by $i \in \{1, 2\}$. $d_{\alpha ik\sigma}^\dagger$ ($d_{\alpha ik\sigma}$) is the creation (annihilation) operator for the electron with momentum $\boldsymbol{k}$ in the electrode i connected to the dot α; $\xi_{\alpha ik}$ denotes the electron energy, while $eV_{\alpha i}$ is the energy shift due to the applied voltage $V_{\alpha i}$ (see Fig. 1). The Coulomb interaction between electrode i and the dot α is represented by the term with parameter $U_{\alpha i}$, whilst the tunnelling of the electron through the junction is described by the third part. The matrix elements $T_{\alpha i}$ are assumed to be independent of spin and momentum. The Coulomb interaction between electrons localized on different dots is described by the term

$$\mathcal{H}_{d-d} = U_{d-d} \sum_{\sigma,\sigma'} n_{t\sigma} n_{b\sigma'}.$$

In general, the currents, which flow through the system, can be calculated using the quantum–mechanical or the semiclassical approach. To calculate the currents in the quantum regime, one should solve simultaneously a quantum kinetic equation and the Poisson equation [8]. The quantum kinetic equation allows us to compute directly the energy distribution of carriers and obtain any other quantity such as the electron density or the current density anywhere within the device. The Poisson equation describes the electrostatic potential due to any charge imbalance within the sample, which accounts for electron–electron interactions in the Hartree approximation. According to the solving procedure described in detail by McLennan *et al.* [8], one has to obtain the equilibrium conduction–band diagram, solving the Poisson equation for the electrostatic potential self–consistently with the equilibrium electron density. After that one should solve the transport equation with the boundary conditions imposed at the contact regions, and then the correction for the electrostatic potential (again from Poisson equation). In general, the correction (due to the charge imbalance arising under bias, together with the associated screening charges) influences the solution of the transport problem. This means that we should iterate between the last two steps until convergence is achieved. It is clearly seen that the calculations in this approach are very difficult and require knowledge of the particular parameters of the system, such as the geometry and the symmetry of the molecular orbital or dot–electrode connection. Fortunately, to describe sequential tunnelling processes and the Coulomb blockade effect, only information about the occupation of the dot is necessary, while the question of how the electron has tunnelled is less important. That is why we propose a simpler, semiclassical, description of the system, in which we include all important electron–electron interactions.

In the model proposed by Hubbard [7], the energy of the on–site Coulomb interaction (∼10 eV) is much larger than the energy of any other. However, in the case of a quantum dot, the interactions are significantly smaller, because of the screening effect, which are of the order of the charging energy of the isolated dot $E_{ch} = (1/2)e^2/C_o \simeq (1/2)U_\alpha$, where C_o is the capacitance of the single, isolated dot. For example, the charging energy of an isolated sphere depends on its diameter r, $E_{ch} = e^2/4\pi\epsilon_o r$ (*i.e.* $E_{ch} \approx 140$ meV for $r \approx 10$ nm, while $E_{ch} \approx 2$ eV for $r \approx 8$ Å). The other interaction energies $U_{\alpha i}$ and

U_{d-d} correspond to the electrostatic energies $(1/2)e^2/C_{\alpha i}$ and $(1/2)e^2/C_{int}$ (where $C_{\alpha i}$ denotes the effective dot–electrode capacitance, while C_{int} is the capacitance between dots), respectively. One can see, that the effective charging energy of the dot connected to the electrodes is smaller, *e.g.* $E_{ch} \approx 50-100$ μeV for the Co dot 14 nm $\times$ 150 nm $\times$ 2.5 μm [9], $E_{ch} \approx 6-40$ meV for an Al dot of less than 10 nm in diameter [10] and $E_{ch} \approx 0.35$ eV for a molecule of C_{60} (diameter $\sim$8 Å) [11].

In our calculation, we assume, that the interaction energy U_α (and corresponding charging energy of the isolated dot) is greater than $U_{\alpha i}$, U_{d-d} and the thermal energy k_BT. It means, that for small voltage drops there can be only one additional electron on each dot and we may neglect the second term in the Hamiltonian $\mathcal{H}_{dot}$. This assumption significantly simplifies the calculation of the electronic transport and the shot noise, and allows understanding of the physical phenomena, which occur in the system. Additionally, we can restrict our consideration to simply the elastic tunnelling processes (we have to neglect the energy dissipation on the dots, which is usually assumed in the SET containing a large metallic dot [12–14]), and also neglect fluctuations of the electronic levels ϵ_α, which can be caused by thermal and electrostatic fluctuations of the environment.

Since we have neglected the dissipative processes on the dot and consider the ideal electrodes, the localized voltage drops occur only on the tunnel barriers, which we have modelled by the resistances $R_{\alpha i}$. Assuming $V_t^g = V_b^g = V_{t1} = 0$ and $C_t^g = C_b^g = 0$ (the case $\neq 0$ we leave for future investigation), from Kirchhoff's laws, one can obtain

$$V_{t1}^{drop} = \frac{C_{t2}C_b}{C^2}V_{t2} + \frac{C_{b1}C_{int}}{C^2}V_{b1} + \frac{C_{b2}C_{int}}{C^2}V_{b2} - \frac{2E_t^c}{e}N_t - \frac{2E_{int}^c}{e}N_b, \tag{2}$$

$$V_{t2}^{drop} = V_{t2} - V_{t1}^{drop}, \tag{3}$$

$$V_{b1}^{drop} = \frac{C_{t2}C_{int}}{C^2}V_{t2} + \frac{C_{int}^2 - C_{b2}C_t - C_{int}C_t}{C^2}V_{b1} + \frac{C_{b2}C_t}{C^2}V_{b2} - \frac{2E_{int}^c}{e}N_t - \frac{2E_b^c}{e}N_b\ , \tag{4}$$

$$V_{b2}^{drop} = V_{b2} - V_{b1}^{drop} - V_{b1}\ , \tag{5}$$

where $C_{\alpha i}$ is the capacitance of the junction between the dot α and the electrode i, $C_\alpha = C_{\alpha 1} + C_{\alpha 2} + C_{int}$ ($\alpha = \{t, b\}$), $C^2 = C_tC_b - C_{int}^2$, and E_α^c is the charging energy of the dot α: $E_t^c = \dfrac{e^2C_b}{2C^2}$, $E_b^c = \dfrac{e^2C_t}{2C^2}$. $E_{int}^c = \dfrac{e^2C_{int}}{2C^2}$ represents the dot–dot interaction energy, V_{t2} denotes the bias voltage in the top SET, $V_{b2} - V_{b1}$ is the bias in the bottom SET, while $-e$ ($e > 0$) and T stand for the electron charge and the temperature, respectively.

Tunnelling processes for an electron in the top ($\alpha = t$) and the bottom ($\alpha = b$) SET through the left ($i = 1$) and the right ($i = 2$) junctions, are described by the net tunnelling rates

$$\gamma_{\alpha i} \sim \frac{1}{R_{\alpha i}e^2} = \frac{2\pi}{\hbar}D_\alpha D_{\alpha i}|T_{\alpha i}|^2,$$

which depend on the tunnel matrix elements $T_{\alpha i}$ and a density of states at the Fermi level on the dot α (D_α), and in the electrode i ($D_{\alpha i}$). The processes are assumed to be small, such that $\hbar\gamma_{\alpha i} \ll k_BT$. This relation implies that the corresponding tunnel resistances $R_{\alpha i}$ are much larger than the quantum resistance $R_Q = h/2e^2$ and the electronic transport is dominated by incoherent, sequential tunnelling processes [13,15], whereas higher–order tunnelling processes (cotunnelling) are neglected. Therefore, one can describe the electronic transport through the system introducing the following master equation:

$$\frac{\mathrm{d}}{\mathrm{d}t}p(N_t, N_b; t) = A(N_t, N_b)p(N_t, N_b; t) + \sum_{\alpha=t,b} B_\alpha^+(N_t, N_b)p(N_t + \delta_{t\alpha}, N_b + \delta_{b\alpha}) + \sum_{\alpha=t,b} B_\alpha^-(N_t, N_b)p(N_t - \delta_{t\alpha}, N_b - \delta_{b\alpha}), \tag{6}$$

where $\delta_{t\alpha}$, $\delta_{b\alpha}$ are the Kronecker's deltas,

$$A(N_t, N_b) = -\sum_{r=\pm}\sum_{\alpha=t,b}\sum_{i=1,2}\Gamma_{\alpha i}^r(N_t, N_b), \tag{7}$$

$$B_i^\pm(N_t, N_b) = \sum_{i=1,2}\Gamma_{\alpha i}^\pm(N_t \pm \delta_{t\alpha}, N_b \pm \delta_{b\alpha})\ , \tag{8}$$

and $p(N_t, N_b; t)$ denotes the probability to find $N_t = 0, 1$ excess electrons on the top dot and $N_b = 0, 1$ excess electrons on the bottom one. The effective tunnelling rates for electrons in the top and the bottom SET, tunnelling to (+) and from (−) the particle level ϵ_α through the junction αi, are given by

$$\Gamma_{\alpha i}^\pm(N_t, N_b) = \gamma_{\alpha i}f_{\alpha i}^\pm(N_t, N_b)\ , \tag{9}$$

where the distribution function

$$f_{\alpha i}^\pm(N_t, N_b) = \left[1 + \exp\left(\pm\frac{\epsilon_\alpha - eV_{\alpha i}^{drop}(N_t, N_b) \mp E_\alpha^c - E_F}{k_BT}\right)\right]^{-1} \tag{10}$$

and E_F denotes the Fermi energy.

The effective tunnelling rates $\Gamma_{\alpha i}^\pm(N_t, N_b)$ and the probabilities $p(N_t, N_b, t)$ determine the tunnelling currents $I_{\alpha i}$. In the stationary state

$$I_{\alpha i} = -e\sum_{N_t,N_b}(-1)^i \times \left[\Gamma_{\alpha i}^+(N_t, N_b) - \Gamma_{\alpha i}^-(N_t, N_b)\right]p_0(N_t, N_b), \tag{11}$$

where the probability $p_0(N_t, N_b)$ is calculated from the master equation (6) with the left hand side equal to zero. In the steady state, one can also determine the average value of any physical quantity X

$$\langle X\rangle = \sum_{N_t,N_b}X(N_t, N_b)p_0(N_t, N_b), \tag{12}$$

where $X(N_t, N_b)$ is the representation of X in the two–dimensional space of states $\{(N_t, N_b)\}$.

To analyze fluctuations in the system we extend the generation–recombination approach [16] for multi–electron channels by a generalization of the method developed for spinless electrons in a SET [17–21]. The time correlation function of the quantities X and Y can be expressed as

$$\langle X(t)Y(0)\rangle = \sum_{N_t',N_b';N_t,N_b} X(N_t',N_b') \times P\left(N_t',N_b';t|N_t,N_b;0\right) Y(N_t,N_b)\, p_0(N_t,N_b). \quad (13)$$

Here, $P(N_t', N_b'; t|N_t, N_b; 0)$ is the conditional probability to find the system in the final state with N_t' and N_b' excess electrons at time t, if there were N_t and N_b excess electrons at the initial time $t = 0$. This probability is determined from the equation (written in the matrix form)

$$\frac{\mathrm{d}\widehat{P}}{\mathrm{d}t} = \widehat{M}\widehat{P} \quad (14)$$

for the time evolution of the conditional probability $P(N_t', N_b'; t|N_t, N_b; 0)$. The tunnel matrix $\widehat{M}$ results from the master equation (6) and depends on $\Gamma_{\alpha i}^{\pm}(N_t, N_b)$. In calculation of the current–current correlation functions, one has to include the self–correlation terms as well [17–21]. According to this procedure the Fourier transform of the charge–charge S_{NN} and polarization–polarization S_{PP} correlation functions are given by

$$S_{\substack{NN\\(PP)}}(\omega) = 4 \sum_{N_t',N_b';N_t,N_b} (N_t' \pm N_b') \times \mathrm{Re}\left[\frac{1}{\mathrm{i}\omega\widehat{1} - \widehat{M}}\right]_{N_t',N_b';N_t,N_b} (N_t \pm N_b) p_0(N_t,N_b)\,, \quad (15)$$

while the current–current correlation function is

$$S_{I_{\alpha i}I_{\beta j}}(\omega) = \delta_{\alpha\beta}\delta_{ij} S_{I_{\alpha i}}^{Sch} + S_{I_{\alpha i}I_{\beta j}}^{c}(\omega), \quad (16)$$

where $\delta_{\alpha\beta}$, δ_{ij} are the Kronecker's deltas, the Schottky value (the frequency independent part) is given by

$$S_{I_{\alpha i}}^{Sch} = 2e^2 \sum_{N_t,N_b} \left[\Gamma_{\alpha i}^{+}(N_t,N_b) + \Gamma_{\alpha i}^{-}(N_t,N_b)\right] p_0(N_t,N_b), \quad (17)$$

and the frequency dependent part has the following form

$$S_{I_{\alpha i}I_{\beta j}}^{c}(\omega) = 4e^2 \sum_{N_t',N_b';N_t,N_b} (-1)^{i+j} \times \left[\Gamma_{\alpha i}^{+}(N_t',N_b') - \Gamma_{\alpha i}^{-}(N_t',N_b')\right] \mathrm{Re}\left[\frac{1}{\mathrm{i}\omega\widehat{1} - \widehat{M}}\right]_{N_t',N_b';N_t,N_b} \times \Big[\Gamma_{\beta j}^{+}(N_t - \delta_{t\beta}, N_b - \delta_{b\beta}) p_0(N_t - \delta_{t\beta}, N_b - \delta_{b\beta}) - \Gamma_{\beta j}^{-}(N_t + \delta_{t\beta}, N_b + \delta_{b\beta}) p_0(N_t + \delta_{t\beta}, N_b + \delta_{b\beta})\Big]. \quad (18)$$

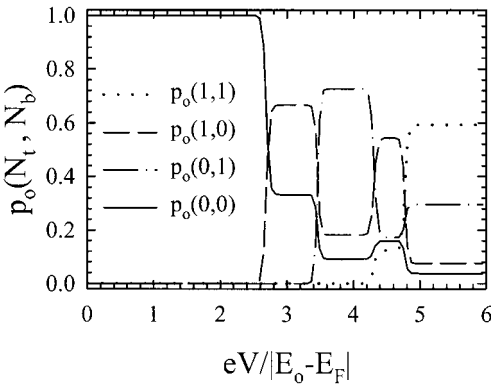

Fig. 2. Voltage dependence of the probability $p_0(N_t, N_b)$. The parameters are: $C_{t1} = 0.4\ aF$, $C_{t2} = 0.2\ aF$, $C_{b1} = 0.15\ aF$, $C_{b2} = 0.25\ aF$, $C_{int} = 0.5\ aF$, C_α^g=0, $\epsilon_t = 0.5|E_0 - E_F|$, $\epsilon_b = |E_0 - E_F|$, $k_BT = 0.01|E_0 - E_F|$, $\gamma_{t1} = \gamma_0$, $\gamma_{t2} = 0.5\gamma_0$, $\gamma_{b1} = 0.8\gamma_0$, $\gamma_{b2} = 0.1\gamma_0$, $V_\alpha^g = V_{b1} = V_{b2} = 0$ and $V_{t2} = V_{b2} = V$. γ_0 is taken as unity in our calculations.

3 Results

3.1 Stationary processes

To characterize the system in the stationary state, we have numerically calculated the bias voltage dependence of the current $I_t = I_{t1} = I_{t2}$ ($I_b = I_{b1} = I_{b2}$) flowing through the top (bottom) SET and the average charge accumulated on each dot, $\langle N_t\rangle$ and $\langle N_b\rangle$. In our model the system can be found in one of the four charge states: $\{(N_t, N_b)\} = \{(0,0),(0,1),(1,0),(1,1)\}$. One can see from Figure 2, that for small voltages, the probability $p_0(0,0)$, that the both dots are empty (*i.e.* without additional electrons) is equal to one, and currents cannot flow through the system (Fig. 3). This is the so–called Coulomb blockade effect. Currents can flow through the system only above some threshold voltages V^{th}, which are different for both transistors (see Fig. 3):

$$V_t^{th} = \frac{C^2}{C_{t2}C_b + C_{b2}C_{int}} \left(\frac{1}{2}E_t^c + \epsilon_t\right), \quad (19)$$

$$V_b^{th} = \frac{C^2}{C_{b2}C_t + C_{t2}C_{int}} \left(\frac{1}{2}E_b^c + \epsilon_b\right). \quad (20)$$

When the voltage V_{t2} exceeds the threshold voltage V_t^{th}, then the current I_t begins to flow through the top transistor. The probability to find an electron on the top dot $p_0(1,0)$ rises, while the probability to find an electron on the bottom dot $p_0(0,1) = 0$ (see Fig. 2). Each the curves in Figures 3a and b have steps, which result from opening new charge channels, (N_t, N_b). These steps are seen clearly only for low temperatures, when the charging energy E_α^c is much larger than the thermal energy k_BT. For higher temperatures they are smeared out. The amplitude of the currents depend on the tunnelling rates $\gamma_{\alpha i}$. When the voltage V_{b2} exceeds the threshold voltage V_b^{th}, then the current I_b begins to flow also through the bottom dot

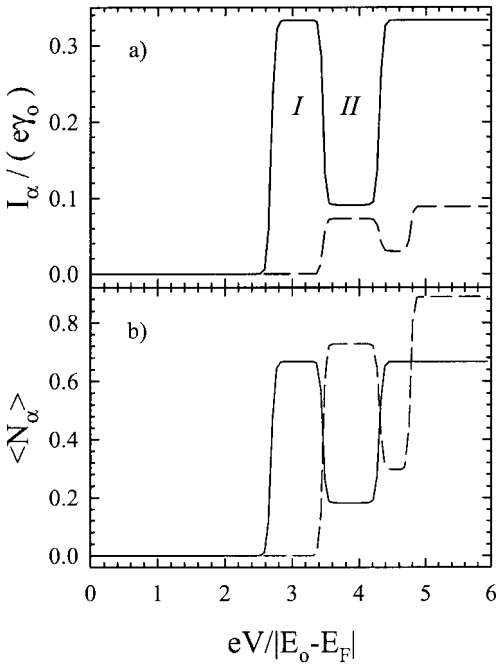

Fig. 3. Current through the top (solid line) and the bottom (dashed line) SET's (a), charge accumulation (b). The parameters are the same as those in Figure 2.

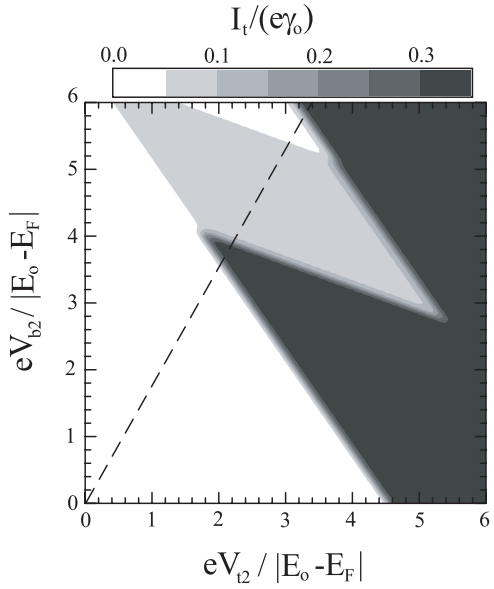

Fig. 4. The contour plot of the current flowing through the top SET I_t as a function of V_{t2} and V_{b2}. The parameters are the same as those in Figure 2.

(Fig. 3). In the case of the tunnelling rate $\gamma_{b2} \ll \gamma_{b1}$, it may lead to quite a large charge accumulation on the bottom dot. If the interaction between the transistors is large (*i.e.* for $C_{int} \geq C_{\alpha i}$), the charge accumulated on the bottom transistor (Fig. 3b) blocks the current channel through the top SET. In effect, a reduction of the current I_t is obtained (area II in Fig. 3a). Since we restrict our consideration to the low temperatures, the distribution functions $f^{\pm}_{\alpha i}$ (from Eq. (10)) are close to zero, or to one, for the plateau, and a drop in the current, I_t, can be calculated analytically. We have derived formulae for the currents flowing through the top (bottom) SET, in the first (I^I_t) and the second (I^{II}_α) plateau regions:

$$I^I_t = e\frac{\gamma_{t1}\gamma_{t2}}{\gamma_{t1}+\gamma_{t2}}, \tag{21}$$

$$I^{II}_t = e\frac{\gamma_{t1}\gamma_{t2}\gamma_{b2}}{\gamma_{t1}\gamma_{b2}+\gamma_{t2}(\gamma_{b1}+\gamma_{b2})}, \tag{22}$$

$$I^{II}_b = e\frac{\gamma_{t2}\gamma_{b1}\gamma_{b2}}{\gamma_{t1}\gamma_{b2}+\gamma_{t2}(\gamma_{b1}+\gamma_{b2})}. \tag{23}$$

Hence, we can quantitatively describe the NDR phenomenon (solid line in Fig. 3) by the ratio

$$NDR = \frac{I^I_t - I^{II}_t}{I^{II}_t} = \frac{\gamma_{b1}\gamma_{t2}}{(\gamma_{t1}+\gamma_{t2})\gamma_{b2}}\,. \tag{24}$$

The largest value of the NDR effect appears for a large asymmetry between the tunnelling rates $\gamma_{b2} \ll \gamma_{b1}$, when the charge accumulation on the bottom dot is large (Fig. 3b).

The results presented in Figures 2 and 3 were calculated in a particular case, when the bias voltage in the bottom transistor was the same as the bias voltage in the top one. In general, however, the voltage drops can be changed independently. The current I_t in the top SET as a function of both the voltage drops, through the top and the bottom transistors, is plotted in Figure 4. Darker (brighter) regions correspond to a larger (smaller) value of the tunnelling current. One can see, that the voltage V_{b2} controls the threshold voltage V^{th}_t and the value of the current in the top transistor, I_t. The V_{b2} can also determine the voltages, for which the NDR effect appears. For example, if one follows the dashed line in Figure 4, *i.e.* when the relation $V_{b2} = 1.75V_{t2}$ is fulfilled, then the NDR effect occurs twice. Here it is worth noting, that double NDR is an important phenomenon, because it allows the building of three–state switches.

3.2 Fluctuation and noise

To characterize the dynamics of the system we performed analysis of the charge and the current noises *versus* the bias voltage and the frequency.

The total charge noise $S_{NN}(\omega = 0)$ for $N = N_t + N_b$, and the polarization noise $S_{PP}(\omega = 0)$ for $P = N_t - N_b$ *versus* voltage are plotted in Figure 5. The characteristics are calculated using formula (15). The correlation functions $S_{NN}(0)$ and $S_{PP}(0)$ are step–like, similarly to the characteristics in the steady state. Changes of the value of the charge and the polarization noises correspond to opening a new charge state (compare Fig. 2 and Fig. 5). Moreover, comparison between Figure 3b and Figure 5 shows that the total charge noise, $S_{NN}(0)$, increases with the increase of the charge accumulation on the top dot. For the top SET, the polarization noise $S_{PP}(0)$ is enhanced in

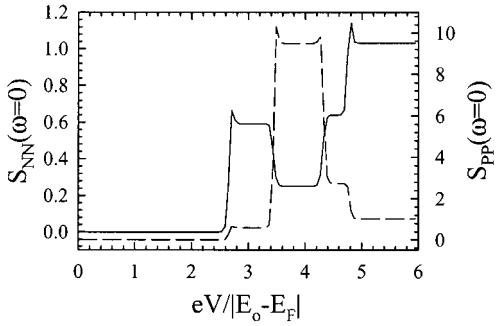

Fig. 5. Charge noise – S_{NN} (solid line) and polarization noise – S_{PP} (dashed line). The parameters are the same as those in Figure 2.

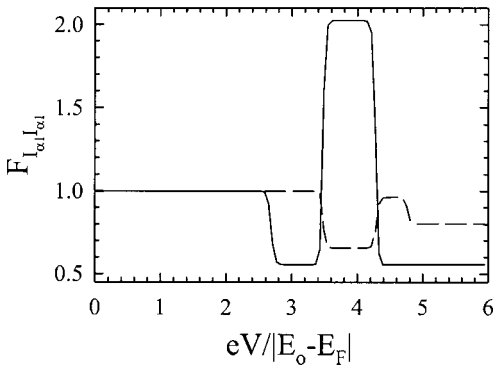

Fig. 6. Fano factor for the top (solid line) and the bottom (dashed line) transistor. The parameters are the same as those in Figure 2.

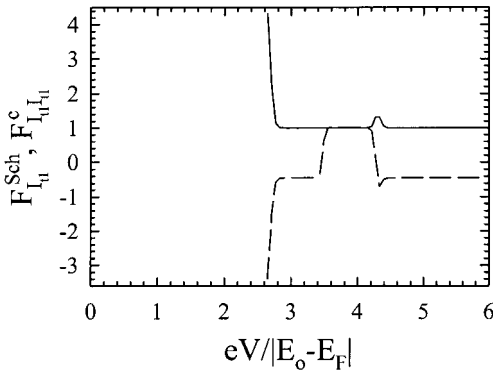

Fig. 7. Contributions to the Fano factor $F_{I_{t1}I_{t1}}$: Schottky noise (solid line) and frequency dependent part (dashed line). The parameters are the same as those in Figure 2.

the NDR and the second plateau regions, while the charge noise $S_{NN}(0)$ is decreased. The polarization fluctuations $S_{PP}(0)$ induced in the NDR and the second plateau regions are one order of magnitude larger than the amplitude of the charge noise $S_{NN}(0)$. However, outside the NDR region, the noise amplitudes are comparable.

The results of numerical calculations of the Fano factors defined as the quotient of the zero frequency current noise and the Poissonian noise $S_{\rm Poisson} = 2eI_\alpha$:

$$\mathcal{F}_{I_{\alpha i}I_{\beta j}} = \frac{S_{I_{\alpha i}I_{\beta j}}(0)}{2eI_\alpha}, \tag{25}$$

are presented in Figure 6. In general, the shot noise is suppressed below the Poissonian value due to the negative correlations between tunnelling electrons, which are generated by Coulomb interactions (the Coulomb blockade effect) [5,17–19].

In the NDR and the second plateau regions (solid line for the top transistor) the zero–frequency current noise is approximately twice as large as the Poissonian noise $S_{\rm Poisson}$. An enhancement of the current noise was recently observed in resonant tunnelling diodes by Iannaccone *et al.* [6]. The enhancement in the resonant tunnelling diodes is obtained because of a shift of the density of states in the well due to electron tunnelling. In our system, however, the nature of the NDR and the enhancement of the shot noise is different.

The current noise in each tunnel junction is the sum of two terms: the frequency independent Schottky noise (Eq. (17)) and the frequency dependent noise (Eq. (18)). For the top transistor, both parts are plotted in Figure 7. The Schottky noise is enhanced at the threshold voltage V_t^{th}. Such behavior is the result of frequent tunnelling of electrons to and from the dot through the less resistive junction (in our case it is the junction $t1$) of the top SET. The analogous process appears in the bottom SET at threshold voltage V_b^{th}. The frequency dependent part is negative for $\omega = 0$. It results from the aforementioned negative correlations between successive tunnelling events and is due to the Coulomb interactions between electrons. Since the Coulomb blockade effect predominates, the current noise is decreased below the Poissonian value $S_{\rm Poisson} = 2eI$ (Fig. 6). However, in the NDR and the second plateau regions, the Fano factors of both coefficients of the current noise are approximately equal to unity and therefore the current noise is super–Poissonian. Since the Fano factor of the Schottky noise is constant (excluding voltages close to V_α^{th}), one can say that the frequency dependent part is responsible for the enhancement of the shot noise.

For voltages related to the second (II) plateau (*e.g.* $V \approx 3.8|E_0 - E_F|/e$), we have found analytical formulae for the current noise $S_{I_{\alpha i}I_{\beta j}}(\omega)$ (Eq. (16)). The Schottky value $S_{\alpha i}^{Sch}$ (Eq. (17)) can be rewritten as

$$S_{\alpha i}^{Sch} = 2eI_\alpha = 2e^2 \frac{\gamma_{\alpha 1}\gamma_{t2}\gamma_{b2}}{\gamma_{t1}\gamma_{b2} + \gamma_{t2}(\gamma_{b1} + \gamma_{b2})}\,. \tag{26}$$

In order to analyze the frequency dependence of the shot noise we perform spectral decomposition. The correlation functions $S^c_{I_{\alpha i}I_{\beta j}}(\omega)$ (as well as $S_{NN}(\omega)$ and $S_{PP}(\omega)$) can be expressed as the sum of the components $S^c_{I_{\alpha i}I_{\beta j}}(\lambda)$ ($S_{NN}(\lambda)$, $S_{PP}(\lambda)$) in the representation of the eigenvalues λ of the tunnel matrix $\widehat{M}$. Each eigenvalue λ corresponds to the relaxation time $\tau = -1/\lambda$. The voltage dependencies of all eigenvalues λ are plotted in Figure 8. Three of them (λ_-, λ_+ and λ_4) are negative, whilst the

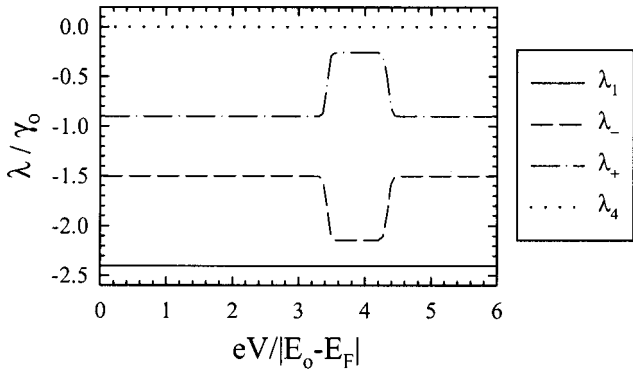

Fig. 8. Voltage dependence of the eigenvalues λ of the matrix $\widehat{M}$. The parameters are the same as those in Figure 2.

fourth is equal to zero ($\lambda_1 = 0$) and corresponds to the stationary solution of the master equation (6). The eigenvalues λ are non–degenerate. In addition, we have found that only terms corresponding to the two eigenvalues λ_- and λ_+ are important. The amplitudes of the $S_{NN}(\lambda_4)$, $S_{PP}(\lambda_4)$ and $S^c_{I_{\alpha i}I_{\beta j}}(\lambda_4)$ are exponentially small (in comparison with the other terms) and can be omitted. We have derived the eigenvalues $\lambda_\pm$ of the matrix $\widehat{M}$ in the second plateau region:

$$\lambda_\pm = \frac{1}{2}\left(-\gamma \pm \sqrt{\gamma^2 - 4[\gamma_{t1}\gamma_{b2} - \gamma_{t2}(\gamma_{b1}+\gamma_{b2})]}\right), \quad (27)$$

where $\gamma = \gamma_{t1}+\gamma_{t2}+\gamma_{b1}+\gamma_{b2}$. After spectral decomposition, the noise $S^c_{I_{\alpha i}I_{\beta j}}(\omega)$ (Eq. (18)) takes on the following form:

$$S^c_{I_{\alpha i}I_{\beta j}}(\omega) = \frac{2eI_\alpha}{\lambda_-^2 - \lambda_+^2}\sum_{r=\pm} r\frac{a_{\alpha i,\beta j} + b_{\alpha i,\beta j}\lambda_r^2}{\omega^2+\lambda_r^2}, \quad (28)$$

where coefficients $a_{\alpha i,\beta j}$ and $b_{\alpha i,\beta j}$ depend only on the tunnelling rates $\gamma_{\alpha i}$ and can be calculated from equation (18):

$$\begin{aligned}
a_{t1,t1} &= a_{t2,t2} = -2\gamma_{t1}\gamma_{t2}(\gamma_{b2}^2 + \gamma_{b1}\gamma_{b2} - \gamma_{t2}\gamma_{b1}) ,\\
b_{t1,t1} &= b_{t2,t2} = 2\gamma_{t1}\gamma_{t2},\\
a_{t2,b2} &= a_{b2,t2} = -\gamma_{t2}^2\gamma_{b1}^2 + \gamma_{b1}\gamma_{b2}^2(\gamma_{t2}-\gamma_{t1}),\\
&\quad +\gamma_{b1}\gamma_{b2}\gamma_{t2}(\gamma_{t1}+\gamma_{t2}+\gamma_{b1}),\\
b_{t2,b2} &= b_{b2,t2} = -(\gamma_{b2}+\gamma_{t2})\gamma_{b1},\\
a_{t1,t2} &= a_{t2,t1} = 2\gamma_{b2}\gamma_{t2}^2\gamma_{b1} + \gamma_{t2}^2\gamma_{b1}(\gamma_{b1}+2\gamma_{t1}),\\
&\quad +\gamma_{b2}^2(\gamma_{t2}^2+\gamma_{t1}^2) ,\\
b_{t1,t2} &= b_{t2,t1} = -\gamma_{t2}^2 - \gamma_{t1}\gamma_{b1} - \gamma_{t1}^2,\\
a_{t2,b1} &= a_{b1,t2} = \gamma_{t2}^2\gamma_{b1}^2 - \gamma_{b2}^2\gamma_{b1}(\gamma_{t2}-\gamma_{b1}),\\
&\quad -\gamma_{t2}\gamma_{b1}\gamma_{b2}(\gamma_{t1}+\gamma_{t2}+\gamma_{b1}),\\
b_{t2,b1} &= b_{b1,t2} = -\gamma_{b1}(\gamma_{t1}+\gamma_{b1}). \quad (29)
\end{aligned}$$

From equations (29) one can see that the current shot noise (Fano factor) depends only on the tunnelling rates $\gamma_{\alpha i}$. The capacitances of the system are not important.

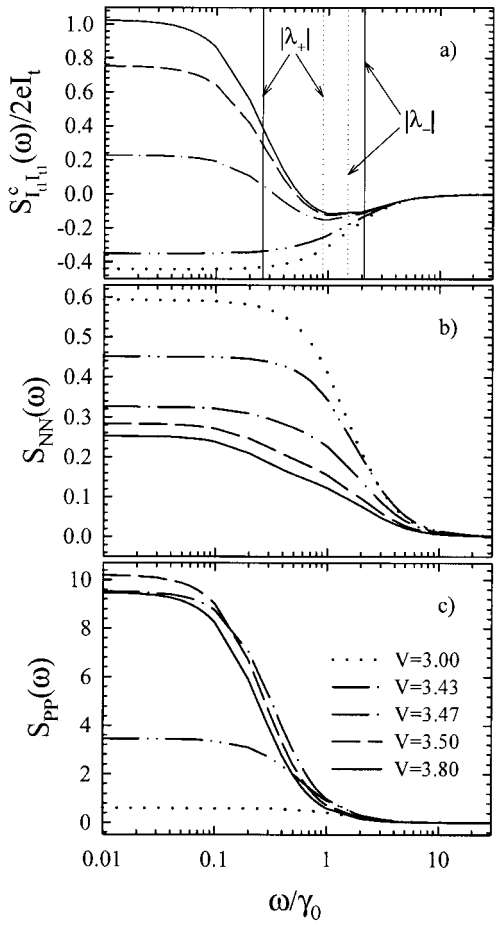

Fig. 9. (a) Fano factor of the current noise $S^c_{I_{t1}I_{t1}}(\omega)$, (b) total charge noise S_{NN} and (c) polarization noise S_{PP} as a function of the frequency ω/γ_0. Thin vertical lines denote values of $\lambda_\pm$ for the voltages $V = 3.0$ (dotted line) and $V = 3.8$ (solid line).The parameters are the same as those in Figure 2.

This result is true only for low temperatures, when the plateau can be clearly seen.

In the limit of low frequency, the shot noise (Eq. (28)) has a simpler form:

$$S^c_{I_{\alpha i}I_{\beta j}}(0) = 2eI_\alpha\frac{a_{\alpha i,\beta j}}{\lambda_-^2\lambda_+^2}\cdot \quad (30)$$

An analysis of equation (30) leads us to the conclusion that the zero frequency current noise $S_{I_{\alpha i}I_{\beta j}}(0)$ depends only on the coefficient $a_{\alpha i,\beta j}$, and can be either super– or sub–Poissonian. For example the shot noise $S_{I_{t1}I_{t1}}(0)$ is enhanced above the Poissonian value under the condition that the tunnelling rate $\gamma_{t2} > \gamma_{b2} + \frac{\gamma_{b2}^2}{\gamma_{b1}}$ (from $a_{t1t1} > 0$, see Eq. (29)). On the other hand, the noise is suppressed below the Poissonian value even in the NDR region.

In Figure 9a, we illustrate the change of the frequency dependent shot noise ($S^c_{I_{t1}I_{t1}}(0)$) whilst going from the first to the second plateau. The thin vertical lines denote the characteristic frequencies $\lambda_\pm$ of the system, which correspond to the extreme slope of the $S^c_{I_{t1}I_{t1}}(\omega)$

for the voltages $V = 3.0|E_0 - E_F|/e$ (dotted line) and $V = 3.8|E_0 - E_F|/e$ (solid line). The power spectrum of the current noise $S^c_{I_{t1}I_{t1}}(\omega)$ (for $V = 3.47, 3.5, 3.8$ in units $|E_0 - E_F|/e$) is positive in the low–frequency regime and negative for higher frequencies. The curves $S^c_{I_{t1}I_{t1}}(\omega)$ (Fig. 9a) are the sum of the two Lorentzian lines, say $S^{c-}_{I_{t1}I_{t1}}(\omega)$ and $S^{c+}_{I_{t1}I_{t1}}(\omega)$, with different relaxation times $\tau_- = -1/\lambda_-$ and $\tau_+ = -1/\lambda_+$, respectively. The high–frequency component $S^{c-}_{I_{t1}I_{t1}}(\omega)$ is negative. It is responsible for the negative correlation in the current noise $S^c_{I_{t1}I_{t1}}(\omega)$ (Fig. 9a). When we are going from the first to the second plateau, then the low–frequency noise $S^c_{I_{t1}I_{t1}}(\omega)$ increases (Fig. 9a). We have found that the enhancement is due to the activation of the amplitude of the noise $S^{c+}_{I_{t1}I_{t1}}(\omega)$ corresponding to the eigenvalue λ_+.

The results for the charge noise are presented in Figure 9b. The noise disappears at high frequencies. The charge correlations corresponding to the eigenvalues λ_- and to the shorter relaxation time τ_-, play dominant roles for the voltages besides NDR and the second plateau regions. One can say that the total charge noise $S_{NN}(\omega)$ is dominated by high frequency tunnelling processes through the junctions of the system.

In the polarization noise, the crucial roles are the processes with the characteristic relaxation time τ_+, corresponding to the slow polarization fluctuations (Fig. 9c). In the NDR and the second plateau regions, the polarization fluctuations are enhanced, their amplitude is approximately two orders of magnitude larger than the amplitude of the total charge noise. Comparisons between Figures 9a, b and c shows that the polarization noise dominated by the low frequency process is responsible for the enhancement of the current noise in the NDR and the second plateau regions. In other words, the current shot noise is super–Poissonian due to the activation of low–frequency fluctuations of the polarization.

4 Final remarks

We have performed theoretical analysis of the steady state transport properties and the shot noise, in the system with two molecular–size SETs connected in parallel. Usually, the opening of new charge channels in the SET leads to current increase; however, in some cases the Coulomb blockade effect can decrease the tunnel currents. In our system, when the coupling is strong, the Coulomb interactions between charges accumulated on both dots are responsible for the NDR phenomenon.

It is well known, that the Coulomb blockade effect in SET's is responsible for the reduction of the current noise up to 1/2 of the Poissonian value. We have shown, however, that interactions between two SETs can also lead to the enhancement of the current noise above the Poissonian value. The spectral analysis of the shot noise shows two main contributions to the current noise: low–frequency polarization fluctuations and high–frequency charge fluctuations. The activation of the polarization noise is responsible for the enhancement of the current noise above the Poissonian value.

Electronic transport measurements concern the stationary currents only [2], and we believe that the power spectrum studies will also be undertaken and will verify our theoretical predictions.

The work in this paper was supported by the State Committee for Scientific Research in the Republic of Poland under Grant No. 2 P03B 087 19.

References

1. J. Chen, M.A. Reed, A.M. Rawlett, J.M. Tour, Science **286**, 1550 (1999)
2. C.P. Heij, D.C. Dixon, P. Hadley, J.E. Moij, Appl. Phys. Lett. **74**, 1042 (1999)
3. Sh. Kogan, *Electronic noise and fluctuations in solids* (Cambridge University Press, 1996)
4. Ya.M. Blanter, M. Büttiker, Phys. Rep. **336**, 1 (2000)
5. H. Birk, M.J.M. de Jong, C. Schönenberger, Phys. Rev. Lett. **75**, 1610 (1995)
6. G. Iannaccone, G. Lombardi, M. Macucci, B. Pellegrini, Phys. Rev. Lett. **80**, 1054 (1998)
7. J. Hubbard, Proc. Roy. Soc. A **276**, 238 (1963)
8. M.J. McLennan, Y. Lee, S. Datta, Phys. Rev. B **43**, 13846 (1991)
9. K. Ono, H. Shimada, Y. Ootuka, J. Phys. Soc. Jpn **66**, 1261 (1997)
10. D.C. Ralph, C.T. Black, M. Tinkham, Phys. Rev. Lett. **74**, 3241 (1995)
11. D. Porath, Y. Levi, M. Tarabiah, O. Millo, Phys. Rev. B **56**, 9829 (1997)
12. D.K. Ferry, S.M. Goodnick, *Transport in Nanostructures* (Cambridge University Press, 1997)
13. G. Schön, in *Quantum Transport and Dissipation*, edited by T. Dittrich, P. Hänggi, G.-L. Ingold, B. Kramer, G. Schön, W. Zwerger, Chap. 3 (Wiley-VCH Verlag, New York, 1998)
14. D.V. Averin, A.N. Korotkov, K.K. Likharev, Phys. Rev. B **44**, 6199 (1991)
15. *Single Charge Tunneling*, Vol. 294 of *NATO Advanced Study Institute, Series B: Physics*, edited by H. Grabert, M.H. Devoret (Plenum, New York, 1992)
16. K.M. van Vliet, J.R. Fassett, in *Fluctuation Phenomena in Solids*, edited by R.E. Burgess (Academic Press, New York, 1965), p. 267
17. A.N. Korotkov, Phys. Rev. B **49**, 10381 (1994)
18. S. Hershfield, J.H. Davies, P. Hyldgaard, C.J. Stanton, J.W. Wilkins, Phys. Rev. B **47**, 1967 (1993)
19. U. Hanke, Yu.M. Galperin, K.A. Chao, N. Zou, Phys. Rev. B **48**, 17209 (1993)
20. U. Hanke, Yu.M. Galperin, K.A. Chao, N. Zou, Phys. Rev. B **50**, 1595 (1994)
21. A. Imamoglu, Y. Yamamoto, Phys. Rev. Lett. **70**, 3327 (1993)